Cluster observations of energetic electron acceleration within earthward reconnection jet and associated magnetic flux rope

A. Vaivads[1], Yu. V. Khotyaintsev[2], A. Retinò[3], H. S. Fu[4], E. A. Kronberg[5], P. W. Daly[6]

[1]Space and Plasma Physics, School of Electrical Engineering and Computer Science, KTH Royal Institute of Technology, Sweden
[2]Swedish Institute of Space Physics, Uppsala, Sweden
[3]Laboratoire de Physique des Plasmas LPP, Centre National de la Recherche Scientifique CNRS, France
[4]School of Space and Environment, Beihang University, Beijing, China
[5]Department of Earth and Environmental Sciences, University of Munich, Munich, Germany
[6]Max Planck Institute for Solar System Research, Göttingen, Germany

Key Points:

- Detailed study of energetic electron acceleration in the braking region of earthward propagating reconnection jet
- Large electron acceleration in the magnetic flux pile-up region and in the turbulent region containing a magnetic flux rope in front of the jet
- The largest energetic electron fluxes are inside the flux rope, probably due to Fermi acceleration process

Corresponding author: A.Vaivads, `vaivads@kth.se`

Abstract

We study acceleration of energetic electrons in an earthward plasma jet due to magnetic reconnection in the Earth magnetotail for one case observed by Cluster. The case has been selected due to the presence of high fluxes of energetic electrons, Cluster being in the burst mode and Cluster separation being around 1000 km that is optimal for studies of ion scale physics. We show that two characteristic acceleration mechanisms are operating during this event. First, significant acceleration is achieved inside the magnetic flux pile-up of the jet, the acceleration mechanism being consistent with betatron acceleration. Second, strong energetic electron acceleration occurs in magnetic flux rope like structure forming in front of the magnetic flux pile-up region. Energetic electrons inside the magnetic flux rope are accelerated predominantly in the field-aligned direction and the acceleration can be due to Fermi acceleration in a contracting flux rope.

1 Introduction

High-speed jets created by the magnetic reconnection process are one of the major source regions of suprathermal/energetic electrons in astrophysical plasmas. The near-Earth space, particularly magnetotail, is an ideal place to make experimental observations of the regions where those electrons are accelerated(Birn et al., 2012; Sitnov et al., 2019). Statistical studies have shown that highest electron fluxes are occurring closer to the Earth where the magnetic field gets more dipolar(Åsnes et al., 2008; Luo et al., 2011). According to observations and numerical simulations one of important driver of electron energization is the reconnection process that allows electron acceleration both close to the reconnection site as well as in the regions of outflow jets(Birn et al., 2012; Hoshino et al., 2001; Imada et al., 2007).

One region of particular importance for the electron acceleration is the region where earthward jets are braking against the dipolar field lines of near-Earth magnetosphere (Khotyaintsev et al., 2011; Malykhin, Grigorenko, Kronberg, & Daly, 2018). Detailed studies of selected events show that magnetic pile-up regions, also called dipolarization fronts, forming in front of the reconnection jets can contain high fluxes of energetic electrons accelerated due to both betatron and Fermi acceleration mechanisms(Fu et al., 2011; Birn et al., 2012; Fu et al., 2013). It has also been shown on an event-case basis that the region where reconnection jets are braking against the dipolar field are associated with high fluxes of energetic electrons (Vaivads et al., 2011; Malykhin, Grigorenko, Kronberg, Koleva, et al., 2018). However, there are still open questions regarding which are the most efficient acceleration processes and what is the relative contribution of the various processes.

Different studies have pointed out that magnetic islands or flux ropes can contribute to the acceleration of electrons. Particularly, a recent study using ARTEMIS data from tailward flows and comparisons with 2D PIC numerical simulations suggested that energetic electrons are correlated to the center of the magnetic islands(Lu et al., 2020). Magnetic flux ropes on much smaller scale associated with energetic electrons has been reported earlier also as seen by Cluster spacecraft (Retinò et al., 2008; Huang et al., 2012; Chen et al., 2008). Detailed MMS observations within a magnetic fluc rope produced by reconnection showed a difference in the acceleration on both sides of the island and identified the betatron acceleration mechanism as the dominant player(Zhong et al., 2020). Statistical studies of magnetic flux ropes have shown that only about one fourth of them show increased fluxes of energetic electrons(Borg et al., 2012). Numerical simulations have shown energetic electron production in kinetic scale flux ropes (Oka, Fujimoto, et al., 2010; Oka, Phan, et al., 2010). The important role of ion-scales magnetic flux ropes for generation of energetic electrons has been shown also in large-scale simulations (Zhou et al., 2018).

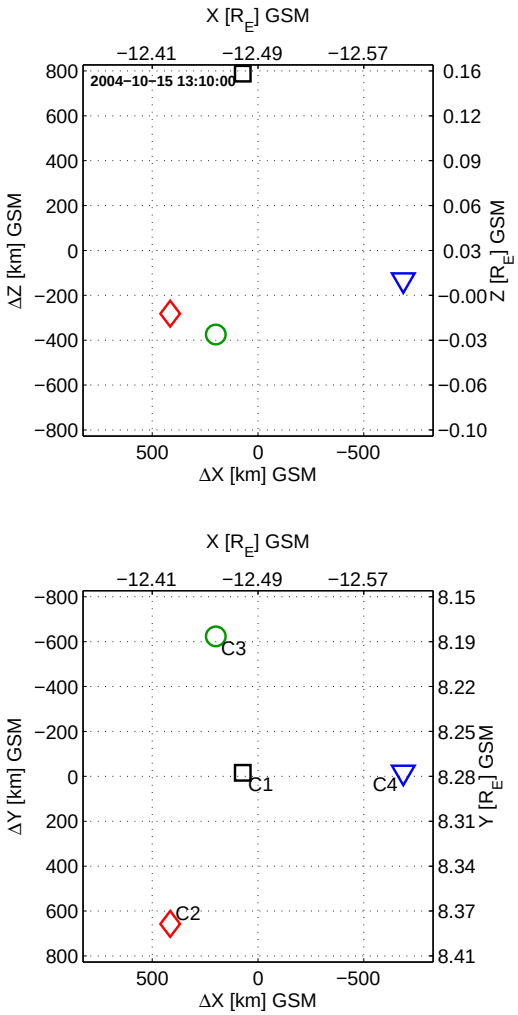

Figure 1. Cluster location and configuration in GSM reference frame.

The reconnection jet fronts can be one of the places of the magnetic island formation. Recent high resolution numerical simulations have shown the process of island formation in front of reconnection jets, however they could not study the energetic electron properties(Lapenta et al., 2015). The experimental observations of such island formation are scarce. In this paper we present a detailed study of a single event showing high fluxes of energetic electrons generated inside kinetic-scale magnetic flux rope in front of the reconnection jet and associated magnetic pile-up region.

2 Observations

We have selected for deeper study one event of high suprathermal/energetic electron fluxes associated with the reconnection jet in the Earth's magnetotail based on several criteria: 1) Cluster is in the magnetotail, 2) the presence of strong energetic electron acceleration, 3) reconnection jet associated with a magnetic flux pile-up region, 4) Cluster separation is comparable to the ion scales allowing us to study microphysics of energetic electron acceleration, 5) Cluster is running in Burst Mode (high telemetry mode), providing the highest resolution data from both field and particle instruments. Based

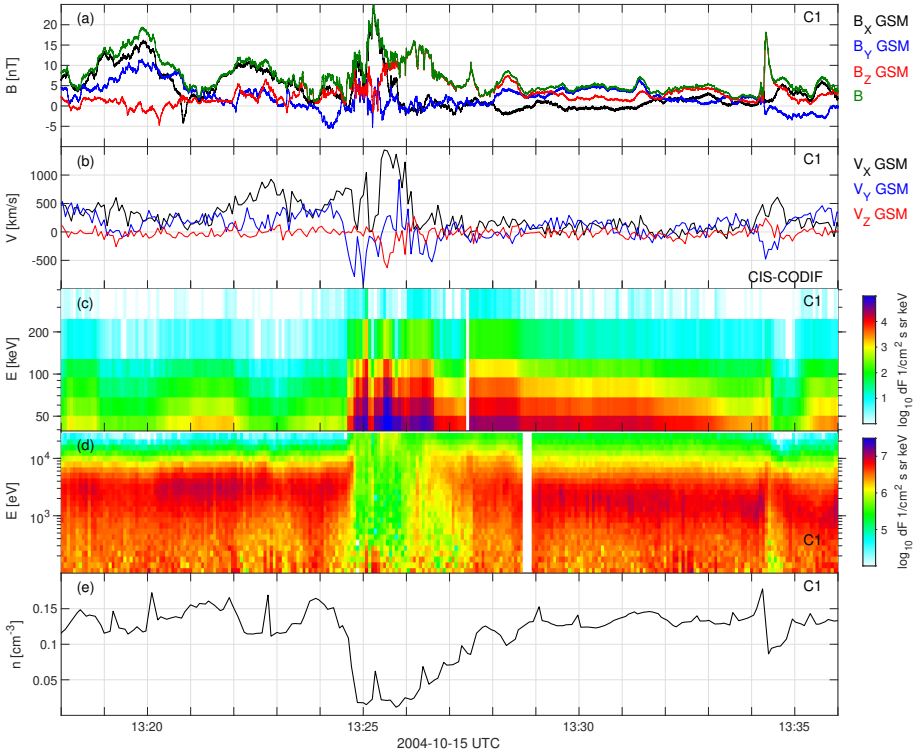

Figure 2. Event overview as seen by C1. (a) Magnetic field in GSM coordinates, (b) ion velocity as measured by the CIS-CODIF instrument, (c) energetic electron differential number flux, measured by RAPID, (d) electron differential number flux, measured by PEACE, (e) electron density measured by PEACE.

on these criteria we could identify several events. For the detailed study presented in this paper we select the event around 2004-10-15 13:26 UT.

During the selected event Cluster is located close to the neutral sheet at [-12.5, 8.3, 0] R_E GSM, see Figure 1. The Cluster separation is ~1000 km which is comparable to a characteristic local ion scale, which is the gyroradius of 10 keV proton in 10 nT field ρ_i ~1400 km. Of particular importance for the paper will be that C4 is located most tailward and C1 is located most northward.

We use measurements of magnetic field (FGM instrument), electric field (EFW), ions (CIS) and electrons (PEACE, RAPID) (Escoubet et al., 1997). During the event Cluster was in the Burst Mode (high-telemetry mode) allowing detailed and high-time resolution measurements of particles and fields. We identify the four Cluster spacecraft as C1, C2, C3 and C4.

Figure 2 shows the large-scale context of the event as seen by Cluster spacecraft C1. During most of the event $|B_X|$ is close to zero or is small in comparison to its expected lobe field value of ~20 nT, see Figure 2a. Thus C1 is located inside the plasma sheet close to the neutral sheet. Similar argument applies to the other Cluster spacecraft (not shown). The plasma sheet can be also identified by the presence of several keV hot thermal electrons, see Figure 2d. Plasma ions show earthward flows throughout the interval, $V_X > 0$ in Figure 2b, being the highest in the beginning of the interval with the peak reaching 1500 km/s at 13:25:30 UT. Around the peak of V_X we observe an increase

in B_Z, and the region of increased B_z (flux pile-up region) continues for a few minutes after the peak in velocity. Also, around the V_X peak we observe a significant density decrease, Figure 2e. All these signatures are characteristic for earthward jets produced by the reconnection tailward of the spacecraft. Figure 2c shows the energetic electron spectrogram, by energetic we mean the electron energies are tens of times larger than the thermal energy of electrons. Very strong increase in energetic electron fluxes is seen in association with the ion jet and magnetic flux pile-up region. The magnetic flux pile-up region and its associated energetic electron generation is the focus of this paper.

There is another smaller magnetic flux pile-up region during the second part of interval in Figure 2. There are ion flows with a localize peak of about 500 km/s around 13:34:30 UT and distinct magnetic flux pile-up associated to this peak. However, there are no associated peak in energetic electron flux. It is interesting to note that the second pile-up region was included in a large statistical study (Fu et al., 2012) analyzing energetic electron acceleration at the dipolarization fronts, while the first one is not. The reason for this is that the second pile-up region has a very distinct and sharp front which was used as a condition for event selection in previous studies (Fu et al., 2012). The first pile-up region does not have such a front, but it is associated with strong energetic electron acceleration. This indicates that many pile-up regions with strong energetic electron generation may be missed by earlier studies of dipolarization fronts due to their complex front structure. We return in the discussion part to the possible reasons why second pile-up region does not show any signs of energetic electron generation.

Figure 3 shows detailed observations of the first magnetic flux pile-up region as seen by all four Cluster spacecraft during a 3 min interval. Figure 3a shows the magnitude of magnetic field. The low values of $|B|$ indicate that spacecraft are inside the plasma sheet close to the neutral sheet. Only during the short interval around 13:25:15 UT C1 is observing B larger than 20 nT indicating that C1 enters into the lobe during that time period. Figure 3b shows that all spacecraft observed magnetic flux pile-up, seen as increase in the B_Z. All spacecraft observe the entering into the pile-up region almost simultaneously consistent with pile-up region passing spacecraft with high speed. However, the exiting of the pile-up region takes much longer time and thus the boundary is moving slowly, consistent with ion velocity in Figure 2. We can also see that C4 is the first that sees the B_Z decrease after the passage of the pile-up region, This is consistent with C4 being the most tailward spacecraft, see Figure 1. Figure 3c shows the sunward velocities (X-component in ISR2 reference frame) estimated from $\mathbf{E} \times \mathbf{B}$-drift and measured by the ion spectrometer. The ISR2 reference frame is individual to each of the satellites, it is close to GSE but has X and Y components in the satellite spin plane. In general $\mathbf{E} \times \mathbf{B}$ velocities are higher than ion drift velocities, consistent with ion instrument not being able to observe all thermal ions due to their high thermal energy which exceeds the maximum energy which can be measured by the CODIF instrument. Figure 3d shows the velocity component in the dawn-dusk direction (ISR2 Y). Large flow in the dawn direction can be seen before the magnetic pile-up. During the peak sunward velocity, there is no significant ISR2 Y-component of velocity. Figure 3e shows the energetic electrons flux observed by C4. There is a general increase of energetic electron flux associated with the sunward flow seen both before and during the magnetic flux pile-up region. However, the peak fluxes are very localized and there can be large change between the measurements performed during the consecutive spacecraft spins (satellite spin is 4 s). The last two panels Figure 3f,g show current and $\mathbf{j} \times \mathbf{B}$ force estimates based on the multi-spacecraft curlometer technique. A significant positive j_Y can be seen in Figure 3f during the first half of the interval, while the current gets week during the second half where the plasma velocity is small and B_Z dominates. Figure 3g shows the $\mathbf{j} \times \mathbf{B}$ force acting on plasma. There is a significant positive $(\mathbf{j} \times \mathbf{B})_X$ during the first half of the interval corresponding to the earthward jet. In the center of interval there is a significant negative $(\mathbf{j} \times \mathbf{B})_Z$ as the spacecraft constellation is slightly above the center of

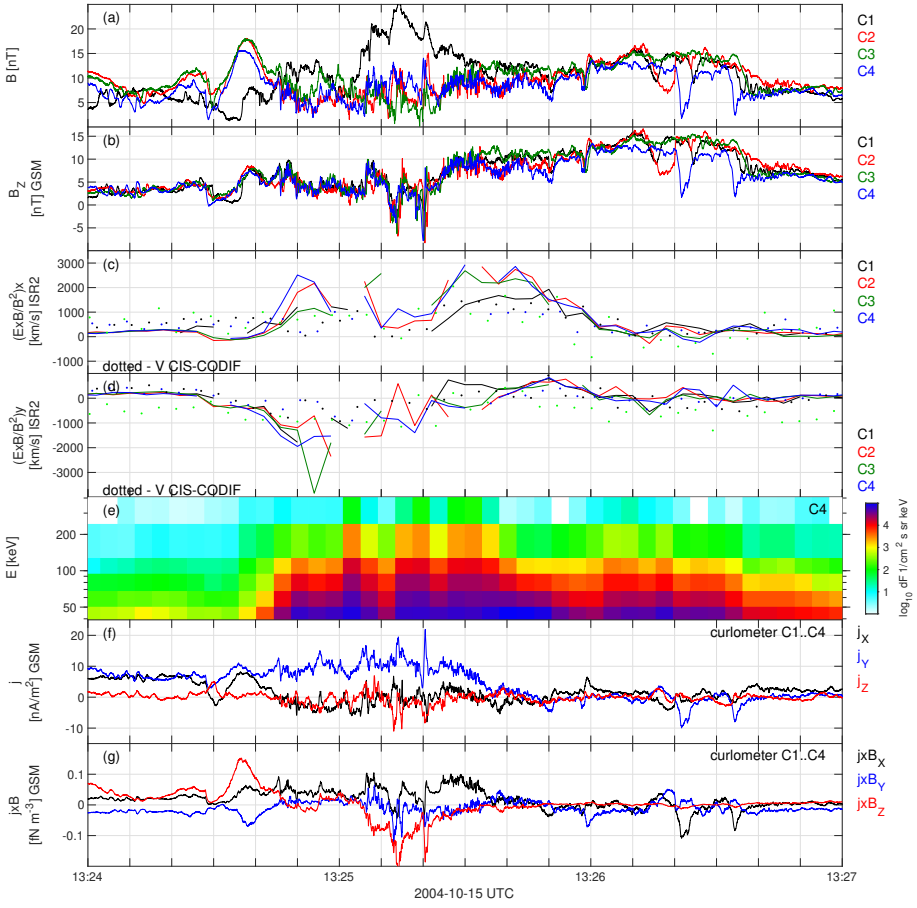

Figure 3. Multi-spacecraft overview. (a) The magnitude of magnetic filed, (b) B_Z GSM, (c) V_X ISR2 from CIS-CODIF measurements and from $\mathbf{E} \times \mathbf{B}$-velocity estimates using electric field measurement, (d) same but for Y ISR2 component, (e) energetic electron differential flux as seen by C4, (f) current estimate based on the curlometer method, (g) $\mathbf{j} \times \mathbf{B}$-force based on the curlometer method.

the current sheet. The negative $(\mathbf{j} \times \mathbf{B})_Y$ in the beginning of the interval is consistent with strong plasma flows in the -Y direction.

Figure 4 shows detailed observations of the pile-up region and energetic electrons as seen by all Cluster spacecraft. Figure 4a shows magnetic field B_Z GSM. The pile-up region is reached around 13:25:30 UT when B_Z reaches steady values of about 10 nT. Next four panels, Figure 4b-e, show the pitch angle distribution of energetic electrons at ~60 keV energy. To understand the details of the energization process, we are plotting the sub-spin resolution data. The electron instrument provides the full 3D distribution during a full spin. However, assuming that electrons are gyrotropic, we can use instantaneous 2D measurements during the spin (subspin resolution) to cover a limited range of pitch-angles. This range will vary during the spin due to varying orientation of $\mathbf{B}$ relative to the 2D plane of the measurement and this variation can be clearly seen in the plot. The grey areas show regions that have not been accessible to the measurement. C1 observes the lowest fluxes because C1 is the furthest away from the center of the current sheet as can be seen from C1 having largest B values in Figure 3a. As adiabatic acceleration mechanisms involve changes in magnetic field magnitude, we overplot the magnitude of

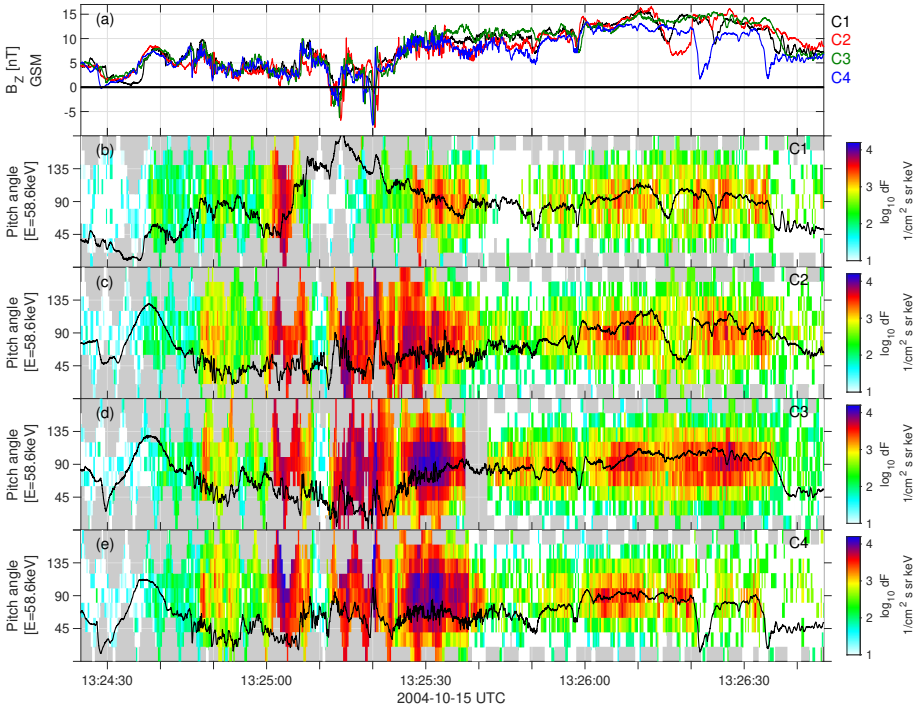

Figure 4. Magnetic pile-up region and energetic electron anisotropies. (a) B_Z in GSM from all Cluster spacecraft, (b-e) pitch angle spectrogram of energetic electrons corresponding to the RAPID channel of 60 keV at subspin resolution, the areas marked in gray correspond to pitch angles not accessible for measurement during that moment of the spin and the white areas correspond to low or zero fluxes.

B (solid line) on top of electron spectrograms. Several important observations can be noted. 1) During the maximum of magnetic pile-up, around 13:26:00-13:26:40, there is a clear increase in energetic electron fluxes and the highest fluxes are close to 90 degree pitch angles. However, this is not the region of the highest fluxes. The highest fluxes are observed in the interval 13:25:00–13:25:40 UT which corresponds to the region before the pile-up and the beginning of the pile-up region. During this time period the highest sunward velocities are observed, see Figure 3c. Inside the beginning of the pile-up region electrons are dominated by fluxes close to 90 degree pitch angles. Before the pile-up region there is no clear pitch-angle dependence and the magnetic field is highly variable. We focus on this region in even more detail.

To better identify the location of the most energetic electrons with respect to the magnetic structure, Figure 5 shows an additional zoom in. Figure 5a shows B_Z GSM and Figure 5b-d show C2-C4 energetic electron spectrograms, those satellites are closest to the current sheet and observe the largest fluxes. The color-scale of the electron spectrograms has been changed to better identify the most energetic electrons. The largest fluxes are seen by C3 and C4. Inside the pile-up region there is a wide region of high flux with the peak at 90 degree pitch angle. However, also at subspin resolution the highest electron fluxes are highly varying. There is another region, just after 13:25:20 UT where very high electron fluxes are briefly (for just a few energy sweeps) observed. In this region the instrument observes the highest instantaneous electron fluxes during the whole event. In the discussion we argue that this region is consistent with being a magnetic flux rope. There are several important observations related to these electrons. 1) Magnetic field

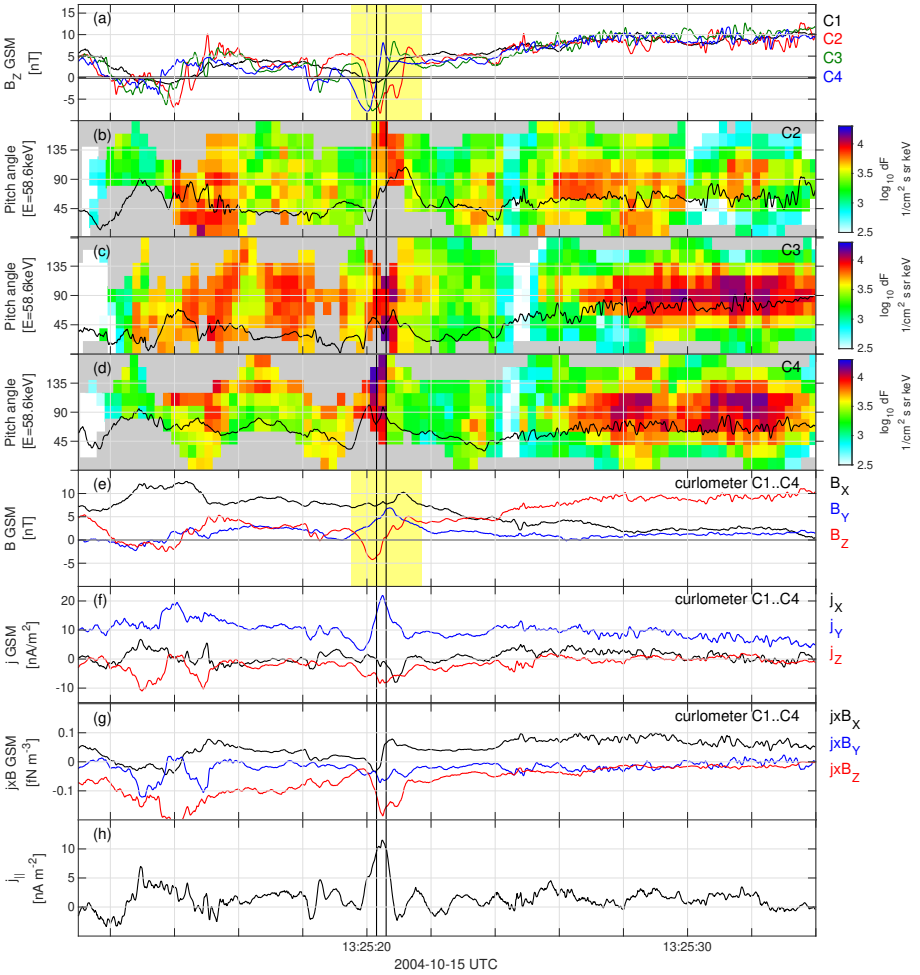

Figure 5. Zoom in around the front of magnetic flux pile-up region. (a) B_Z in GSM from all Cluster spacecraft, the region of negative/positive variation is marked yellow. (b-d) C2-C4 pitch angle spectrogram of energetic electrons corresponding to the RAPID channel of 60 keV at subspin resolution, the areas marked in gray correspond to pitch angles not accessible for measurement during that moment of the spin. (e-f) Observations based on all four spacecraft measurements: (e) average magnetic field, (f) current estimate based on curlometer method, (g) $\mathbf{j} \times \mathbf{B}$ force based on curlometer method, (h) current parallel to the ambient magnetic field.

shows a negative-positive bipolar B_Z variation near the region of the highest fluxes, the region is marked yellow in Figure 5a. 2) The peak fluxes on C3 and C4 coincide with the center of bipolar B_Z variation. The center of the bipolar structures where B_Z crosses zero (going from negative to positive values) are marked by solid lines for C3 and C4 respectively. 3) The magnitude of magnetic field shows a dip at the location of the highest fluxes at C3 and C4. 4) The highest fluxes of electrons are not necessary centred around 90 degree pitch angle. There even seems to be a tendency for electrons to be more field-aligned than perpendicular. 5) C2 sees lower electrons fluxes, there is no dip in magnetic field magnitude and also the bipolar structure is less clear. We will discuss later that these observations are consistent with the presence of a magnetic flux rope.

To better characterize this magnetic structure in Figure 5e-h we plot various quantities computed using 4-point measurements by Cluster. Figure 5e shows the average magnetic field. It can be seen that during the time of the bipolar B_Z variation there is also a strong B_Y component. Such a B_Y component is consistent with core field of magnetic flux rope as we will show in the discussion part. Figure 5f shows the current, the peak in the current is coinciding with the region of highest energetic electron fluxes. Figure 5g shows $\mathbf{j} \times \mathbf{B}$ force. During the whole interval $(\mathbf{j} \times \mathbf{B})_X$ is mainly positive, and around the highest fluxes one can see a bipolar negative/positive signature in $(\mathbf{j} \times \mathbf{B})_X$. Finally, Figure 5h shows the current parallel to the average magnetic field $j_{||}$, and we can see a strong peak in $j_{||}$ coinciding with the location of high energetic electron fluxes.

3 Discussion

Based on the observations presented above we can make the overall interpretation of the event. During the time interval 13:25-13:26 we see high-speed earthward jet that reaches above 1000 km/s in ion data and more than 2000 km/s in $\mathbf{E} \times \mathbf{B}$-velocity. This is consistent with an observation of an earthward reconnection jet. The energies of thermal ions reach above the energy range of the CODIF instrument used to estimate the velocity moment and therefore the ion velocity shows values lower than the $\mathbf{E} \times \mathbf{B}$ velocity. During about 2 min following the peak of the jet velocity we observe a region where B_Z is dominating, with the B_Z values of the order of 10 nT. We interpret this as the magnetic flux pile-up region driven by the jet. However, during the last part of the B_Z-dominated region V_X decreases to small values and even reverses the sign. This suggests that spacecraft are on the dipolar field lines close to the jet braking region. Thus the spacecraft are located in the right region to observe the incoming magnetic pile-up region driven by the reconnection jet, how it brakes due to the near Earth dipolar-like field and how the jet driven magnetic pile-up becomes part of the near Earth dipolar field. Additional support for this hypothesis comes from the j_Y observations, see Figure 3. In the beginning of the interval j_Y is strong and positive both before and in the beginning of the magnetic flux pile-up region. This is consistent with spacecraft located in the thin current sheet in the beginning of the interval followed by reconnection jet driven magnetic flux pile-up. As the jet brakes and its velocity decreases to zero also j_Y value goes to zero consistent with spacecraft being on dipolar field lines. Finally, on the exit boundary of dipolar like field region j_Y is negative as expected when being on the outer region of dipolar field lines. Thus, we are observing the whole chain consisting of the onset of fast reconnection jet, followed by jet braking and spacecraft location close to the dipolar field lines where the jet brakes.

During the interval of jet we observe significantly increased energetic (40-400keV) electron fluxes. The Cluster separation of ∼1000 km comparable to characteristic ions scales allows for detailed exploration of energetic electron acceleration. We observe that there are several mechanisms in play providing the acceleration. In the pile-up region the dominant acceleration is occurring at close to 90 degree pitch angles, with the highest fluxes observed at 13:25:30 UT simultaneous with the detection of the highest jet velocities. Thus, this region is most probably a magnetic flux pile-up region driven by the reconnection jet and what we observe is the betatron acceleration as has been reported in earlier studies (Khotyaintsev et al., 2011; Fu et al., 2011). However, high fluxes of energetic electrons are also observed in the turbulent region in front of the pile-up region, as can be clearly seen in Figure 4 and Figure 5. Closer inspection of data in Figure 5 shows that this turbulent region contains the highest electron fluxes during the whole event (observed during a short time interval around 13:25:20 UT).

Multi-pacecraft observations allow to clearly identify the structure of the region with the highest electron fluxes at 13:25:20 UT. The magnetic field observations are consistent with it being a flux-rope-like structure: a negative-positive B_Z variation for earthward moving structure, converging $\mathbf{j} \times \mathbf{B}$ force, strong parallel current in the center of

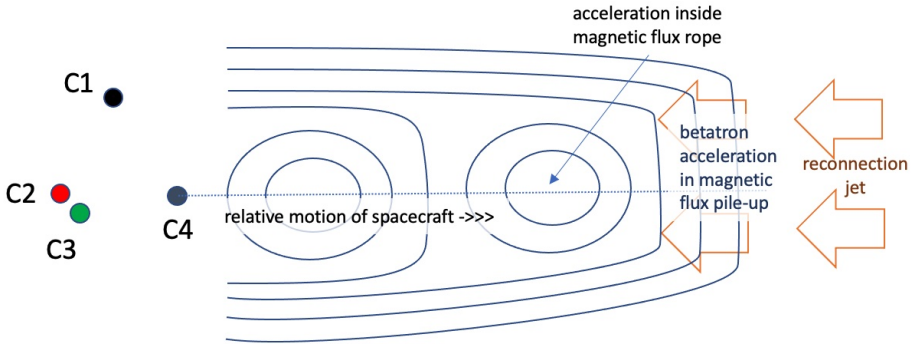

Figure 6. Simplified sketch showing the location of Cluster spacecraft with respect to the current sheet and how they cross the magnetic island and magnetic flux pile-up region.

the structure and a significant core field B_Y. The characteristic cross-section of the flux rope is of the order of the spacecraft separation (ion scales). This is observed both in the X-direction and Z-direction. In the X-direction the two spacecraft separated in X-direction, C2 and C4, simultaneously observe peak values of B_Z of opposite sign consistent with C2-C4 separation being comparable to the flux rope size. In the Z-direction, C1 is separated by ∼1000 km from the other 3 spacecraft, and while C1 sees lobe field values the other 3 spacecraft are still near the center of the current sheet; this is also consistent with the flux-rope scale being comparable to the spacecraft separation. Figure 6 summarizes in a simplified sketch the characteristic separation of spacecraft in comparison to the thickness of the current sheet and the size of magnetic island and illustrates how the spacecraft cross the flux rope.

There have been studies showing presence of high fluxes of energetic electrons in kinetic-scale magnetic islands in the thin current sheet close to the reconnection onset (Retinò et al., 2008; Huang et al., 2012). Both studies show that the highest electron fluxes where detected in the center of magnetic island, while the island was embedded into a thin reconnecting current sheet. When it was possible to measure pitch angle distribution, it was concluded that main acceleration is of energetic electrons at perpendicular direction to the magnetic field. The study by Retinò et al. (2008) also analyzed the pitch-angle distribution and found the highest fluxes for electrons close to 90 degree pitch angles suggesting that they can be energized by the betatron mechanism. Similarly, there is a case study using the MMS observations of energetic electrons inside an ion-scale magnetic island with perpendicular acceleration of electrons (Zhong et al., 2020). Here, we show that magnetic islands can also form in front of the magnetic pile-up region driven by the reconnection jet. In addition, we show that other acceleration mechanisms than betatron acceleration can be at play in the center of the magnetic island. This is related to the fact that we observe the dominant acceleration in filed-aligned direction, and not in the perpendicular direction as expected for the betatron mechanism.

There can be several possible electron acceleration mechanisms inside the flux rope. One is the direct acceleration by the parallel electric field (Pritchett, 2006). The presence of the strong parallel current in the center of the flux rope suggest that there should be also strong parallel fields forming leading to acceleration of electrons in the anti-parallel direction. The presence of parallel fields inside the flux ropes is indirectly supported by observations of electron holes inside the ropes (Khotyaintsev et al., 2010). There is some indication in data, see Figure 5, that C4 which looks in the anti-parallel direction detects the highest fluxes, however, there are too few data points to make a solid conclusion. It is also seen, that C3 that is looking predominantly in the parallel direction also sees in-

creased electron fluxes. Thus there should be additional acceleration mechanisms in play, such as wave-particle interaction or Fermi acceleration in contracting flux rope (Drake et al., 2006). Possible importance of the Fermi acceleration in magnetic flux ropes has been demonstrated also in recent 2D numerical simulations of magnetic reconnection (Arnold et al., 2021). Those simulations show that in case of not too large guide field, which is the case for the magnetotail reconnection, magnetic flux ropes can provide efficient acceleration of energetic electrons. Such a Fermi acceleration mechanism could work also in our case. First, the size of the cross-section of magnetic flux rope most probably is decreasing because flux rope should be gone once the jet pile-up region hits the near Earth dipolar field. Thus the decrease of the cross-section effectively leads to contraction of field lines with a following Fermi acceleration. Secondly, in 3D the flux rope should have a finite length in the direction along the core of the flux rope, corresponding to out-of-plane direction in 2D plots of a magnetic island. In such a case the initial build-up of the flux-rope's core field efficiently corresponds to shortening the length of the field line between the ends of the flux rope. If there are trapped electrons inside the flux rope then this shortening of the field lines will again effectively lead to Fermi acceleration. Thus, both mechanisms separately or in combination can lead to Fermi acceleration inside the flux rope that we observe.

The few detailed case studies of electron acceleration inside flux ropes clearly show that more than one acceleration mechanism can be at play and more studies are needed to understand the relative importance of all those mechanisms. In addition, an important question remain of the relative importance of energetic electron acceleration mechanisms due to acceleration inside the magnetic pile-up region and the turbulent region in front of the jet, including magnetic flux ropes. This requires further statistical studies.

Finally, we discuss the second pile-up region that we mentioned discussing Figure 2 and on which we zoom in Figure 7. The magnetic flux pile-up as seen in Figure 7a has very sharp and clear B_Z increase, there is a significant up to 500 km/s earthward V_X component, see Figure 7b, and as such this event has passed the criteria for earlier dipolarization front studies. However, in comparison to the first pile-up region, this event shows very low flux levels of high energy electrons, see Figure 7c,e. The thermal electron population shown in Figure 7d shows that spacecraft are in the plasma sheet, with relatively small changes in the properties of the electron population. Also density observations in Figure 2e show that density varies inside the jet and the pile-up region but stays close to the surrounding values which is in contrast to the first pile-up region that shows very low densities. One possible explanation might be that the electrons in this second flux pile-up region were initially accelerated at a reconnection site different from the one associated to the first pile-up region and associated to different plasma sheet source electrons. However, we find this unlikely since the two pile-up regions are observed with about 10 minutes time differences during which the overall plasma sheet conditions around the reconnection site should have not changed substantially. Instead, our interpretation is that the second pile-up region is associated to a local flow enhancement which cant still be driven by a reconnection jet and jet braking, as for the first pile-up region, but it is not the reconnection jet itself. This interpretation is supported by the V_Y and $\mathbf{j} \times \mathbf{B}$ force observations, see Figure 7b,g. The V_Y is larger than the V_X and the $\mathbf{j} \times \mathbf{B}$ force in $-Y$ direction, consistent with the pile-up region pushing the plasma in front of it in the $-Y$ direction. This sideways motion can be generated by an incoming jet as it brakes or interacts with another reconnection jet ahead of it, and it pushes surrounding plasma sideways. Such scenario was recently suggested by observations of two consecutive reconnection jets, where the trailing jet had a V_Y much larger than V_X while for the leading jet the largest velocity was V_X (Catapano et al., 2021). Inside the second pile-up region there is some energetic electron energization in perpendicular direction, see Figure 7e, that is most probably caused by the betatron acceleration. However, following the arguments above, it is likely that such energetic electrons come from the pile-up of the lo-

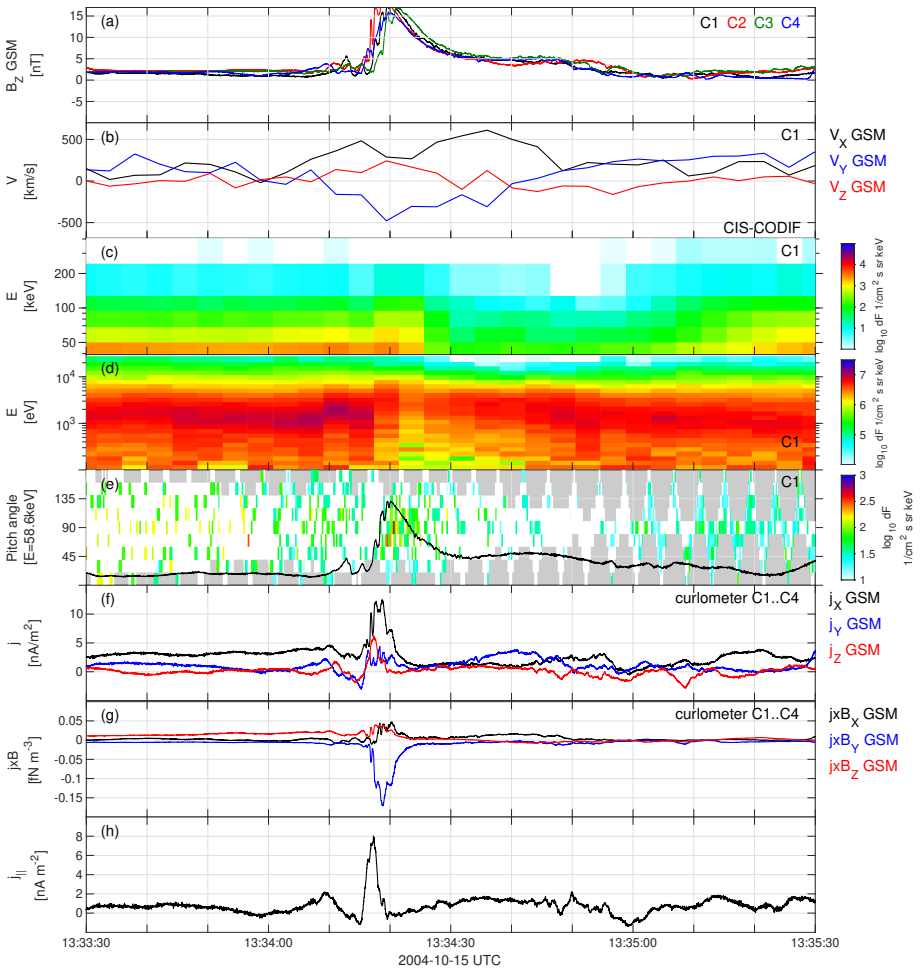

Figure 7. Second magnetic flux pile-up region. (a) B_Z in GSM, (b) plasma velocity in GSM, (c) high energy electron differential number flux, (d) electron differential number flux, (f) current in GSM based on curlometer method, (g) $\mathbf{j} \times \mathbf{B}$-force in GSM, (h) current parallel to the ambient magnetic field.

cal plasma sheet plasma which has lower fluxes of energetic electrons compared to those with the reconnection jet itself. For this reason, the overall fluxes of energetic electrons stay small and this second pile-up region is less important for energetic electron generation compared to the case where the piling-up plasma comes directly from the reconnection site with preexisting high flux levels of energetic electrons, which is the case for the first pile-up region. The highest fluxes of energetic electrons in the magnetic flux pile-up and jet braking regions would then be expected for jets produced by lobe reconnection, as has been suggested also earlier in e.g. Vaivads et al. (2011). Although less important for electron acceleration, the boundary in front of the second pile-up region shows strong parallel current, see Figure 7h, suggesting that this kind of pile-up regions can be important for field aligned coupling to the ionosphere.

4 Summary and conclusions

We present a detailed case study of energetic electron acceleration observed in the region where an earthward reconnection jet reaching up to 2000 km/s brakes close to the near-Earth dipolar-like field. We use data from Cluster spacecraft separated by ∼1000 km that is comparable to the characteristic ion scales (gyroradius of thermal ions). Such separation scale is well suited for applying multi-spacecraft methods to estimates current and $\mathbf{j} \times \mathbf{B}$ force on characteristic ion kinetic scales in the region. We show that the energetic electrons are accelerated both in the magnetic flux pile-up region of the jet mainly through betatron acceleration, as well as in a turbulent region in front of the jet. Inside the turbulent region we can clearly identify a magnetic flux rope or magnetic island-like structure that shows the highest fluxes of energetic electron during the whole event. The highest acceleration region coincides with the center of the flux rope where we also observe the largest current during the event, including the largest field-aligned current. The energetic electrons inside the flux rope have the highest fluxes in the field-aligned directions consistent with being accelerated by either parallel electric field or Fermi acceleration due to contraction of the magnetic island. This event clearly demonstrates the importance of turbulent regions, including flux-rope-like structures, in front of reconnection jets in the acceleration of energetic electrons. In addition, we compare the event with the second magnetic flux pile-up region observed during the same interval but showing much lower fluxes of energetic electrons. The second pile-up region is most probably formed due to local flow enhancement in the plasma sheet and does not plasma coming directly from the reconnection site. We conclude that for highest electron energization it is important that the pile-up region is forming from plasma coming from the reconnection site with preexisting high levels of energetic electrons.

Acknowledgments

Cluster data are downloaded from Cluster Science Archive https://csa.esac.esa.int/csa-web/. We acknowledge the Cluster instrument CIS, EFW, FGM, PEACE, RAPID teams. AV acknowledges support from Swedish Research Council, grant 621-2013-4309. YK acknowledges support from the Swedish National Space Agency grant 139/18. EK is supported by German Research Foundation (DFG) under number KR 4375/2-1 within SPP "Dynamic Earth". PWD is supported by the Deutches Zentrum für Luft- und Raumfahrt (DLR) under grant 50 OC 1602.

References

Arnold, H., Drake, J. F., Swisdak, M., Guo, F., Dahlin, J. T., Chen, B., ... Shen, C. (2021, March). Electron Acceleration during Macroscale Magnetic Reconnection. *Physical Review Letters*, *126*(13), 135101. doi: 10.1103/PhysRevLett.126.135101

Åsnes, A., Friedel, R. W. H., Lavraud, B., Reeves, G. D., Taylor, M. G. G. T., & Daly, P. (2008). Statistical properties of tail plasma sheet electrons above 40 keV. *Journal of Geophysical Research: Space Physics*, *113*(A3). doi: 10.1029/2007JA012502

Birn, J., Artemyev, A. V., Baker, D. N., Echim, M., Hoshino, M., & Zelenyi, L. M. (2012, November). Particle Acceleration in the Magnetotail and Aurora. *Space Science Reviews*, *173*(1), 49–102. doi: 10.1007/s11214-012-9874-4

Borg, A. L., Taylor, M. G. G. T., & Eastwood, J. P. (2012, May). Observations of magnetic flux ropes during magnetic reconnection in the Earth's magnetotail. *Annales Geophysicae*, *30*(5), 761–773. doi: 10.5194/angeo-30-761-2012

Catapano, F., Retinò, A., Zimbardo, G., Alexandrova, A., Cohen, I. J., Turner, D. L., ... Burch, J. L. (2021, February). In Situ Evidence of Ion Acceleration between Consecutive Reconnection Jet Fronts. *The Astrophysical Journal*, *908*(1), 73. doi: 10.3847/1538-4357/abce5a

Chen, L.-J., Bhattacharjee, A., Puhl-Quinn, P. A., Yang, H., Bessho, N., Imada, S., ... Georgescu, E. (2008, January). Observation of energetic electrons within magnetic islands. *Nature Physics*, *4*(1), 19–23. doi: 10.1038/nphys777

Drake, J. F., Swisdak, M., Che, H., & Shay, M. A. (2006, October). Electron acceleration from contracting magnetic islands during reconnection. *Nature*, *443*(7111), 553–556. doi: 10.1038/nature05116

Escoubet, C., Schmidt, R., & Goldstein, M. (1997, January). CLUSTER – SCIENCE AND MISSION OVERVIEW. *Space Science Reviews*, *79*(1), 11–32. doi: 10.1023/A:1004923124586

Fu, H. S., Cao, J. B., Khotyaintsev, Y. V., Sitnov, M. I., Runov, A., Fu, S. Y., ... Huang, S. Y. (2013). Dipolarization fronts as a consequence of transient reconnection: In situ evidence. *Geophysical Research Letters*, *40*(23), 6023–6027. doi: 10.1002/2013GL058620

Fu, H. S., Khotyaintsev, Y. V., André, M., & Vaivads, A. (2011, August). Fermi and betatron acceleration of suprathermal electrons behind dipolarization fronts. *Geophysical Research Letters*, *38*, L16104. doi: 10.1029/2011GL048528

Fu, H. S., Khotyaintsev, Y. V., Vaivads, A., André, M., Sergeev, V. A., Huang, S. Y., ... Daly, P. W. (2012, December). Pitch angle distribution of suprathermal electrons behind dipolarization fronts: A statistical overview. *Journal of Geophysical Research (Space Physics)*, *117*, A12221. doi: 10.1029/2012JA018141

Hoshino, M., Mukai, T., Terasawa, T., & Shinohara, I. (2001). Suprathermal electron acceleration in magnetic reconnection. *Journal of Geophysical Research: Space Physics*, *106*(A11), 25979–25997. doi: 10.1029/2001JA900052

Huang, S. Y., Vaivads, A., Khotyaintsev, Y. V., Zhou, M., Fu, H. S., Retinò, A., ... Pang, Y. (2012). Electron acceleration in the reconnection diffusion region: Cluster observations. *Geophysical Research Letters*, *39*(11). doi: 10.1029/2012GL051946

Imada, S., Nakamura, R., Daly, P. W., Hoshino, M., Baumjohann, W., Mühlbachler, S., ... Rème, H. (2007). Energetic electron acceleration in the downstream reconnection outflow region. *Journal of Geophysical Research: Space Physics*, *112*(A3). doi: 10.1029/2006JA011847

Khotyaintsev, Y. V., Cully, C. M., Vaivads, A., André, M., & Owen, C. J. (2011, April). Plasma Jet Braking: Energy Dissipation and Nonadiabatic Electrons. *Physical Review Letters*, *106*(16), 165001. doi: 10.1103/PhysRevLett.106.165001

Khotyaintsev, Y. V., Vaivads, A., André, M., Fujimoto, M., Retinò, A., & Owen, C. J. (2010, October). Observations of Slow Electron Holes at a Magnetic Reconnection Site. *Physical Review Letters*, *105*, 165002. doi: 10.1103/PhysRevLett.105.165002

Lapenta, G., Markidis, S., Goldman, M. V., & Newman, D. L. (2015, August). Secondary reconnection sites in reconnection-generated flux ropes and reconnection fronts. *Nature Physics*, *11*(8), 690–695. doi: 10.1038/nphys3406

Lu, S., Artemyev, A. V., Angelopoulos, V., & Pritchett, P. L. (2020, June). Energetic Electron Acceleration by Ion-scale Magnetic Islands in Turbulent Magnetic Reconnection: Particle-in-cell Simulations and ARTEMIS Observations. *The Astrophysical Journal*, *896*(2), 105. doi: 10.3847/1538-4357/ab908e

Luo, B., Tu, W., Li, X., Gong, J., Liu, S., des Roziers, E. B., & Baker, D. N. (2011). On energetic electrons (>38 keV) in the central plasma sheet: Data analysis and modeling. *Journal of Geophysical Research: Space Physics*, *116*(A9). doi: 10.1029/2011JA016562

Malykhin, A. Y., Grigorenko, E. E., Kronberg, E. A., & Daly, P. W. (2018, December). The Effect of the Betatron Mechanism on the Dynamics of Superthermal Electron Fluxes within Dipolizations in the Magnetotail. *Geomagnetism and Aeronomy*, *58*(6), 744–752. doi: 10.1134/S0016793218060099

Malykhin, A. Y., Grigorenko, E. E., Kronberg, E. A., Koleva, R., Ganushkina, N. Y., Kozak, L., & Daly, P. W. (2018, May). Contrasting dynamics of electrons and protons in the near-Earth plasma sheet during dipolarization. *Annales Geophysicae*, *36*(3), 741–760. doi: 10.5194/angeo-36-741-2018

Oka, M., Fujimoto, M., Shinohara, I., & Phan, T. D. (2010). "Island surfing" mechanism of electron acceleration during magnetic reconnection. *Journal of Geophysical Research: Space Physics*, *115*(A8). doi: 10.1029/2010JA015392

Oka, M., Phan, T.-D., Krucker, S., Fujimoto, M., & Shinohara, I. (2010, April). ELECTRON ACCELERATION BY MULTI-ISLAND COALESCENCE. *The Astrophysical Journal*, *714*(1), 915–926. doi: 10.1088/0004-637X/714/1/915

Pritchett, P. L. (2006). Relativistic electron production during guide field magnetic reconnection. *Journal of Geophysical Research: Space Physics*, *111*(A10). doi: 10.1029/2006JA011793

Retinò, A., Nakamura, R., Vaivads, A., Khotyaintsev, Y., Hayakawa, T., Tanaka, K., ... Cornilleau-Wehrlin, N. (2008). Cluster observations of energetic electrons and electromagnetic fields within a reconnecting thin current sheet in the Earth's magnetotail. *Journal of Geophysical Research: Space Physics*, *113*(A12). doi: 10.1029/2008JA013511

Sitnov, M., Birn, J., Ferdousi, B., Gordeev, E., Khotyaintsev, Y., Merkin, V., ... Zhou, X. (2019, June). Explosive Magnetotail Activity. *Space Science Reviews*, *215*(4). doi: 10.1007/s11214-019-0599-5

Vaivads, A., Retinò, A., Khotyaintsev, Y. V., & André, M. (2011, October). Suprathermal electron acceleration during reconnection onset in the magnetotail. *Annales Geophysicae*, *29*(10), 1917–1925. doi: 10.5194/angeo-29-1917-2011

Zhong, Z. H., Zhou, M., Tang, R. X., Deng, X. H., Turner, D. L., Cohen, I. J., ... Burch, J. L. (2020). Direct Evidence for Electron Acceleration Within Ion-Scale Flux Rope. *Geophysical Research Letters*, *47*(1), e2019GL085141. doi: 10.1029/2019GL085141

Zhou, M., El-Alaoui, M., Lapenta, G., Berchem, J., Richard, R. L., Schriver, D., & Walker, R. J. (2018). Suprathermal Electron Acceleration in a Reconnecting Magnetotail: Large-Scale Kinetic Simulation. *Journal of Geophysical Research: Space Physics*, *123*(10), 8087–8108. doi: 10.1029/2018JA025502